

In situ and remote sensing signature of meddies east of the mid-Atlantic ridge

I. Bashmachnikov,¹ F. Machín,² A. Mendonça,¹ and A. Martins¹

Received 18 July 2008; revised 21 February 2009; accepted 9 March 2009; published 19 May 2009.

[1] Mediterranean Water eddies (meddies) are thought to play an important climatic role. Nevertheless, their dynamics are not sufficiently known because of difficulties encountered in their observation. Though propagating below the main thermocline, a number of pieces of evidence of sea surface manifestation of meddies are collected. The present work is based on joint in situ and altimetry data analyses to prove that the meddies can be followed with remote sensing data for long periods of time. The in situ observations are based on data from an oceanographic cruise, which crossed three meddies, and reanalysis of historical data sets, including RAFOS floats paths. Suggested methodology permitted us to obtain uninterrupted tracks for several meddies for a period from several months to more than 2 years. It was found that the dynamically calm region to the north of the Azores current presents favorable conditions for meddy tracking. The meddy surface signal may become shattered and difficult to follow during interaction with a strong dynamic structures (the Azores current/surface vortexes) or peaking topography. Theoretical considerations support the observations and lead to the conclusion that the dynamic signature of meddies at the sea surface is an intrinsic property of meddy dynamics.

Citation: Bashmachnikov, I., F. Machín, A. Mendonça, and A. Martins (2009), In situ and remote sensing signature of meddies east of the mid-Atlantic ridge, *J. Geophys. Res.*, 114, C05018, doi:10.1029/2008JC005032.

1. Introduction

[2] Mediterranean Water eddies (meddies) represent warm salty anticyclonically rotating lenses of the modified Mediterranean Water (MW). In the subtropical NE Atlantic meddies typically have horizontal dimensions between 40 and 150 km, and, in vertical, may have one or two cores situated at 700–900 m and at 1000–1200 m. Close to the Iberian coast, their salt and temperature anomalies often exceed 1 practical salinity unit (psu) and 4°C, respectively, but tend to decrease as the meddy progresses away from the generation region. The core of a meddy is typically highly mixed and characterized by low potential vorticity [Richardson *et al.*, 2000].

[3] Meddies are generated through instability of the Mediterranean underwater current at the Iberian continental slope and the Corringe bank, and then propagated mainly westward or southwestward at middepth gradually losing their heat and salt contents to the surrounding water. Because of their high stability meddies are met thousands of kilometers away from the generation region (Figure 1) and are quite frequent features in the NE Atlantic [Richardson *et al.*, 1989; Richardson and Tychensky, 1998; Iorga and Lozier, 1999; Siedler *et al.*, 2005]. They are thought to play an important climatic role, through maintenance of a substantial portion of

the observed MW salt flux into the ocean. Richardson *et al.* [1989], Arhan *et al.* [1994], and Bower *et al.* [1997], using independent data and analyses techniques, estimated that about 15 to 20 meddies are generated on a single year. The associated salt transport may support up to 50% of the observed MW salt flux. At the same time, their observations were concentrated at the southern and central parts of the Iberian Peninsula and did not cover some important regions of meddy formation, as Portimão canyon or Gorringer bank [Serra and Ambar, 2002]. Having analyzed a number of hydrographical sections from the Iberian basin, Maze *et al.* [1997] did not find any stable westward advection patterns west of 12°W, thus, concluding that 100% of the MW salt flux is related to meddy transport. This agrees with the results by Shapiro and Meschanov [1996], who also noted that some of the MW flux around the northern flank of the Josephine seamount can equally be related to advection.

[4] The wide range of the estimates above is partly a result of uncertainty in number of meddies generated per year, as well as, insufficient knowledge of their life histories and propagation patterns. The establishment of an in situ observational network is impeded by the comparatively small spatial scales of the eddies, consequently their remote detection might be helpful. In fact, although propagating below the main thermocline, meddies often have a clear surface signature (Table 1). The last column of Table 1 shows that meddies surface dynamic signal in most cases exceeds 50% of that in the core region at middepth. If this signature is sufficiently stable, remote sensing techniques can become a useful tool to track the meddies.

¹Institute of Marine Research, Department of Oceanography and Fisheries, University of the Azores, Horta, Faial, Azores, Portugal.

²Institut de Ciències del Mar, CSIC, Barcelona, Spain.

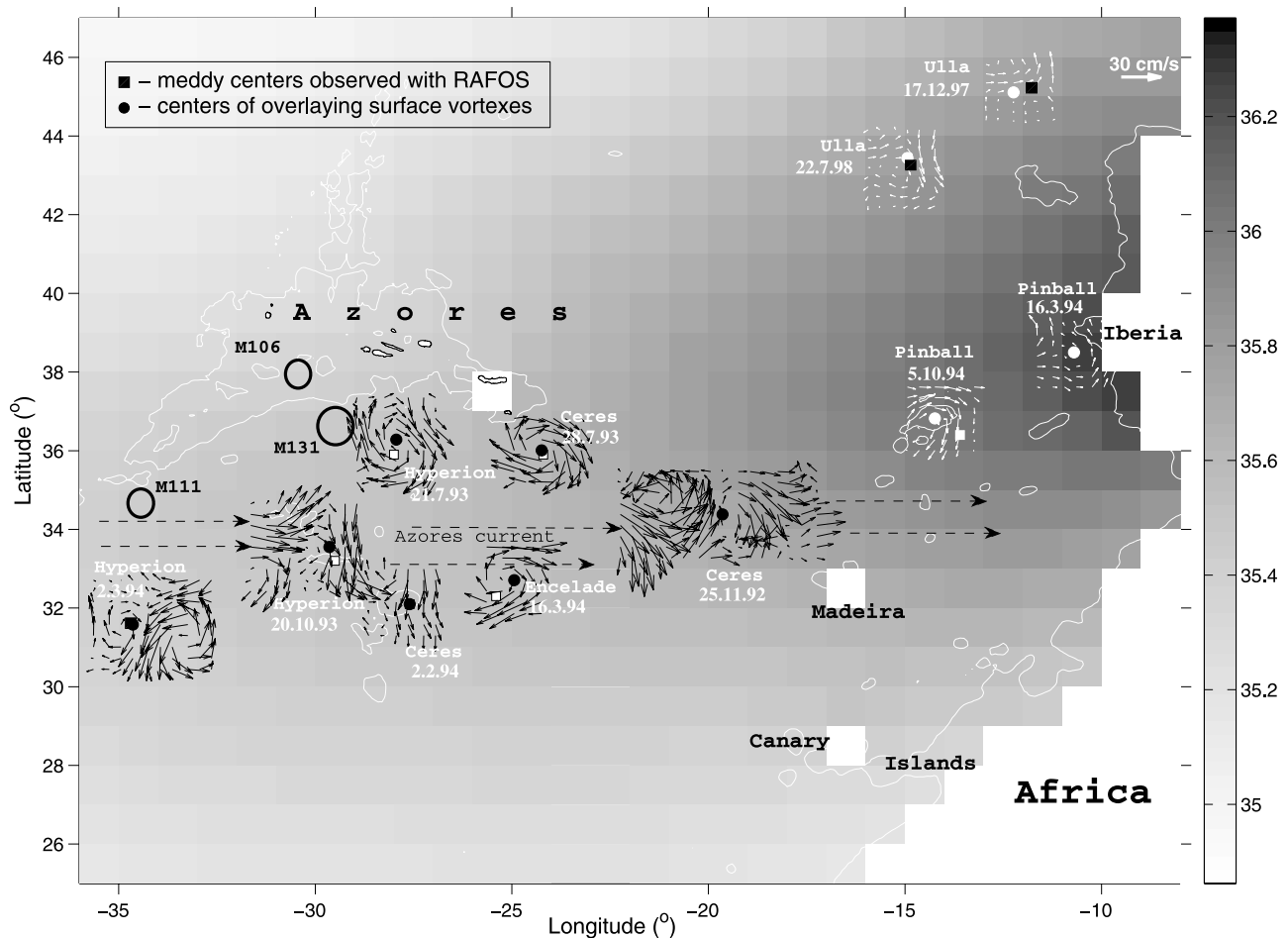


Figure 1. Mediterranean Water (MW) salt tongue at 1000 m [Antonov *et al.*, 2006]. Color scale represents water salinity. Bathymetry is represented with 2000 m depth contour (white line). Large white squares mark the center positions of some meddies from RAFOS float trajectories for the dates specified (see also Tables 1 and 2). Black/white arrows are the altimetry-derived currents for the same period (the reference vector is also shown). Black/white dots represent remotely tracked center positions of the corresponding vortices. Black squares are the result of the exact correspondence of the remote/in situ derived centers. Dashed straight lines represent the approximate position of the AzC jet. Black empty circles mark the positions of three meddies observed during OPALINA cruise.

[5] The idea was first expressed by Käse and Zenk [1987], who detected over a meddy anticyclonic looping trajectories of surface satellite tracked drifters. Afterward, the results were supported by numerical modeling [Käse *et al.*, 1989]. Later, Stammer *et al.* [1991], using Geosat altimetry data, was able to follow several meddies in the Iberian basin. The strongest one could be tracked for more than 1 year. Oliveira *et al.* [2000] showed that all four Iberian basin meddies, detected with in situ data during 1994, were also visible in the Topex/Poseidon (T/P) ground tracks. On along-track sea level profiles the meddies could be seen as positive bell-like sea level anomalies with about 10 cm of amplitude. For some of the tracks the anomalies resided at the same place for up to 20–30 days, and could be repeatedly resampled. The signal was exceptionally clear even when a track crossed a meddy 50–60 km away from the center. At the very side of a meddy (90–100 km away), the meddy surface signature, still visible, lowered to the level of the background noise and was difficult to detect. Tournadre [1990] estimated that the

probability to see an eddy from altimeter data depends on satellite cross-track distance, repetitivity of the track, as well as, eddy diameter and propagation speed. The author predicted that the joint missions of Geosat and T/P are able to detect 95% of 130 km rings and 60% of 100 km rings, propagating at the speed of 2–10 cm s⁻¹, with 80% probability. The similar computations, accepted as Archiving, Validation, and Interpretation of Satellite Oceanographic data (AVISO) recommendations, state that robust detection of mesoscale structures can be made with at least three altimetry satellites on orbit (with both, T/P and ERS orbit parameters), while one satellite is generally insufficient for mesoscale eddy detection (<http://www.aviso.oceanobs.com/en/altimetry/multi-satellites/index.html>). This means, that a robust detection of meddies is possible at least since 2000, when data from T/P, ERS and GFO satellites could be merged.

[6] In the present work we establish observational evidence that most of the historical meddies did have a surface signal sufficiently stable and pronounced to be followed

Table 1. Observations of Surface Signatures of Meddies^a

Reference	Meddies' Names	Instrumentation Showing Deep and/or Surface Signatures	R (km)	V_c (cm s ⁻¹)	V_s (cm s ⁻¹)	V_s/V_c (%)
<i>At the Formation Region (Iberian Basin)</i>						
<i>Käse et al.</i> [1989]	model	Numerical model	<50	10	7	70
<i>Stammer et al.</i> [1991]	A	CTD, SLA, mooring	N.D.	5	3	60
	B	CTD, SLA, mooring	N.D.	7	2	29
	D	CTD, SLA, mooring	N.D.	12	4	33
<i>Pingree and Le Cann</i> [1993]	Smeddy	CTD, XBT, PF, SST	13	20	8	40
<i>Schultz Tokos et al.</i> [1994]	Aska (A)	CTD, RAFOS, SF	17	23	12	56
	B1	CTD, RAFOS, SF	25	25	10	40
	B2	CTD, RAFOS, SF	30	31	18	58
<i>Oliveira et al.</i> [2000]	A1	RAFOS, SF, SLA, SST	18	23	23	100
	A2	RAFOS, SF, SLA, SST	37	20	17	83
	A3(Pinball)	RAFOS, SF, SLA, SST	17	23	23	100
<i>Paillet et al.</i> [2002]	Ulla	CTD, XBT, LADCP, RAFOS, DDB, SF	15	17.5	7.5	43
<i>Away From the Formation Region</i>						
<i>Tychensky and Carton</i> [1998] (south of the Azores)	Hyperion	CTD, XBT, SF, SLA	<60	22.5	18	80
	Ceres	CTD, XBT, SF, SLA	<50	23	30	130 ^b
<i>Le Cann et al.</i> [2005] (Azores-Biscay Rise)	Enclade	CTD, XBT, SF, SLA	<70	16	6	38
	A2	CTD, RAFOS, PF, SF	<40	15	13	87
Mean values			21	18	13	72

^a R is the radius of maximum azimuthal velocity at the depth of the meddy core (tentative values), V_c is the maximum azimuthal velocity value at the meddy core, and V_s is the maximum azimuthal velocity at the sea surface (meddy signal). CTD, conductivity-temperature-depth profilers; SLA, sea level anomalies; N.D., no data available; XBT, expandable bathythermograph profilers; PF, profiling floats; SST, sea surface temperature; SF, surface floats; LADCP, Lowered Acoustic Doppler Profiler; DDB, deep-drogued floats.

^bMaximum at the surface is due to surface vortex, aligned with the meddy.

with altimetry for long periods of time, as well, as discuss the background conditions which should be met for successful continuous tracking.

2. Materials and Methods

[7] Within the framework of Ocean Dynamics and related Productivity of the Northeast Subtropical Atlantic Near the Azores region using ENVISAT, ERS, SeaWiFS, NOAA, and in situ data (OPALINA) (PDCTE/CTA/49965/2003) project, an oceanographic cruise aboard the R/V *Arquipelago* was accomplished in August 2005 (Figure 2). The region of observations is in the vicinity of the mid-Atlantic ridge (MAR), between the Azores archipelago and the Azores current (AzC). Thirty six conductivity-temperature-depth profilers (CTD) casts were made down to 2000 m depth, the data further processed with the standard SBE processing procedure. During the cruise three meddies were identified as positive temperature-salinity anomalies and a negative potential vorticity (PV) anomaly. Here, Ertel PV is computed as [Pedlosky, 1987; Pingree and Le Cann, 1993]:

$$PV = N^2/g * (\zeta + f), \quad (1)$$

where g is gravity acceleration, N is buoyancy frequency and f is Coriolis parameter. For typical azimuthal current speeds in meddies of around 20 cm s⁻¹ and core radius of 20 km, relative vorticity $\zeta \sim 1*10^{-5}$ s⁻¹ $\ll f \sim 8*10^{-5}$ s⁻¹, and to the first order of accuracy the PV can be estimated as the buoyancy frequency normalized by $g*f$.

[8] From the CTD casts geostrophic currents were computed, using an inverse box model technique. The method permits to compute absolute geostrophic velocity fields

consistent with both the thermal wind equation and conservation of water properties, as mass, salt, etc. [Wunsch, 1996]. Water properties are assumed to be preserved inside each of the selected isoneutral density layers [Jackett and McDougall, 1997], presented in Figure 3, as well as in the domain as a whole. The basic formulation of the mass conservation equation is:

$$\iint_A \rho v_r dx dy + \iint_A \rho v_o dx dy = 0, \quad (2)$$

where ρ is the density field, A is the area between selected density layers and hydrographic stations. In the equation, the geostrophic velocity field is divided into a reference level velocity (v_o) and a velocity relative to this level (v_r). The reference level is chosen as the layer with expected minimum (but nonzero) current velocity. In absence of other information, v_o is computed to compensate relative transport imbalances within the water column. Large v_o are considered to result from ageostrophic component of the flow, for which the thermal wind equation fails. To avoid the related errors, v_o values should be limited to a certain range. Evaluation of possible errors in v_o , e.g., possible accuracy to which the conservation equation could be satisfied, is performed through *a priori* estimation of the covariance of the noise (R_{nn}) and the covariance of the unknowns (R_{xx}). R_{xx} is estimated through the variance in the direct velocity measurements in the eastern North Atlantic [Müller and Siedler, 1992; Machin et al., 2006], which for the reference level $\gamma_{ref} = 27.922$ (the lower interface for Mediterranean Water) gives a quite small value of $(0.02)^2$ m² s⁻². In this case our data shows an AzC transport of 10 ± 1 Sv,

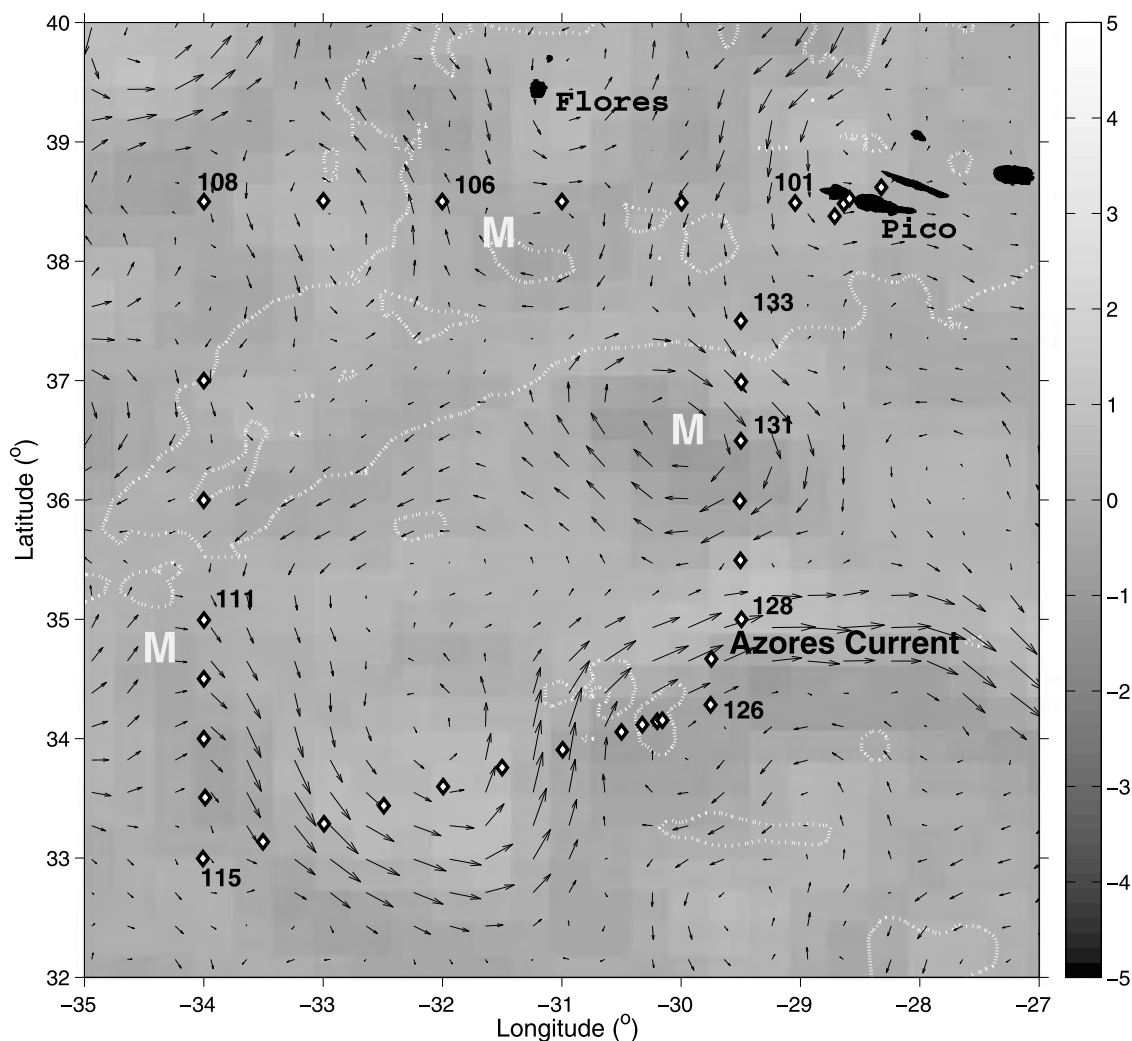


Figure 2. CTD stations of OPALINA cruise (diamonds) overlaid on AVISO altimetry-derived geostrophic currents centered at 17 August 2005. The scale is relative vorticity in 10^{-5} s^{-1} . The suggested meddies' positions are marked with letter "M." White dotted lines represent the 2000 m bathymetry contours. The Azores islands are also shown.

corresponding well to the estimates in [Siedler and Onken, 1996]. As a sensitivity test, we have tried another reference level located at $\gamma_{ref} = 27.200$ (the lower interface of North Atlantic Central water). This results in the residuals of one order higher: $(0.23)^2 \text{ m}^2 \text{ s}^{-2}$, and small AzC transport of $5 \pm 5 \text{ Sv}$. Thus, from the two reference levels, only $\gamma_{ref} = 27.922$ is acceptable. Similarly, the noise uncertainty in the salt anomaly equation is computed as a function of the noise uncertainty in the mass and salt variability equations [Ganachaud, 2003]. In mass equations R_{mn} can be estimated as $(2.2 \cdot 10^9)^2 \text{ kg}^2 \text{ s}^{-2}$, which indicates that the noise could be the same order as the mass transports in the region, and the results of mass conservation will have comparatively low reliability.

[9] The in situ data are supplemented with AVISO altimetry data set (AVISO data available at <http://las.aviso.oceanobs.com/las/servlets/dataset>). In the data set, the absolute dynamic topography is produced by adding time-independent mean dynamic topography to the sea level anomalies from the corrected altimeter measurements. Geo-

strophic currents are computed from the sea level regular grid, obtained by objective space-time interpolation of various satellite tracks. The resultant regular space-time grid has 1/3 of degree mesh interval and weekly time step. The spatial-temporal resolution is good enough to trace surface signals of meddies. The meddy tracing is done with the method of "crawling squares," which proved to be rather stable in tracing corresponding altimetry anomalies [Bashmachnikov et al., 2009]. The method derives the next (or previous) meddy position as a local minimum of the second derivative of sea level height (SLH), not more than one grid point away from the one obtained at a given time step. Using the second derivative, instead of SLH, allows incorporation in the computations of five SLH grid points (in zonal and meridional directions), instead of one. This ensures that we follow some integral part of the structure and adds to the stability of the track. Dynamically, second derivatives from SLH can be regarded as a proxy for relative vorticity. We also consider the situation, when at a certain moment the meddy surface signal fails to appear,

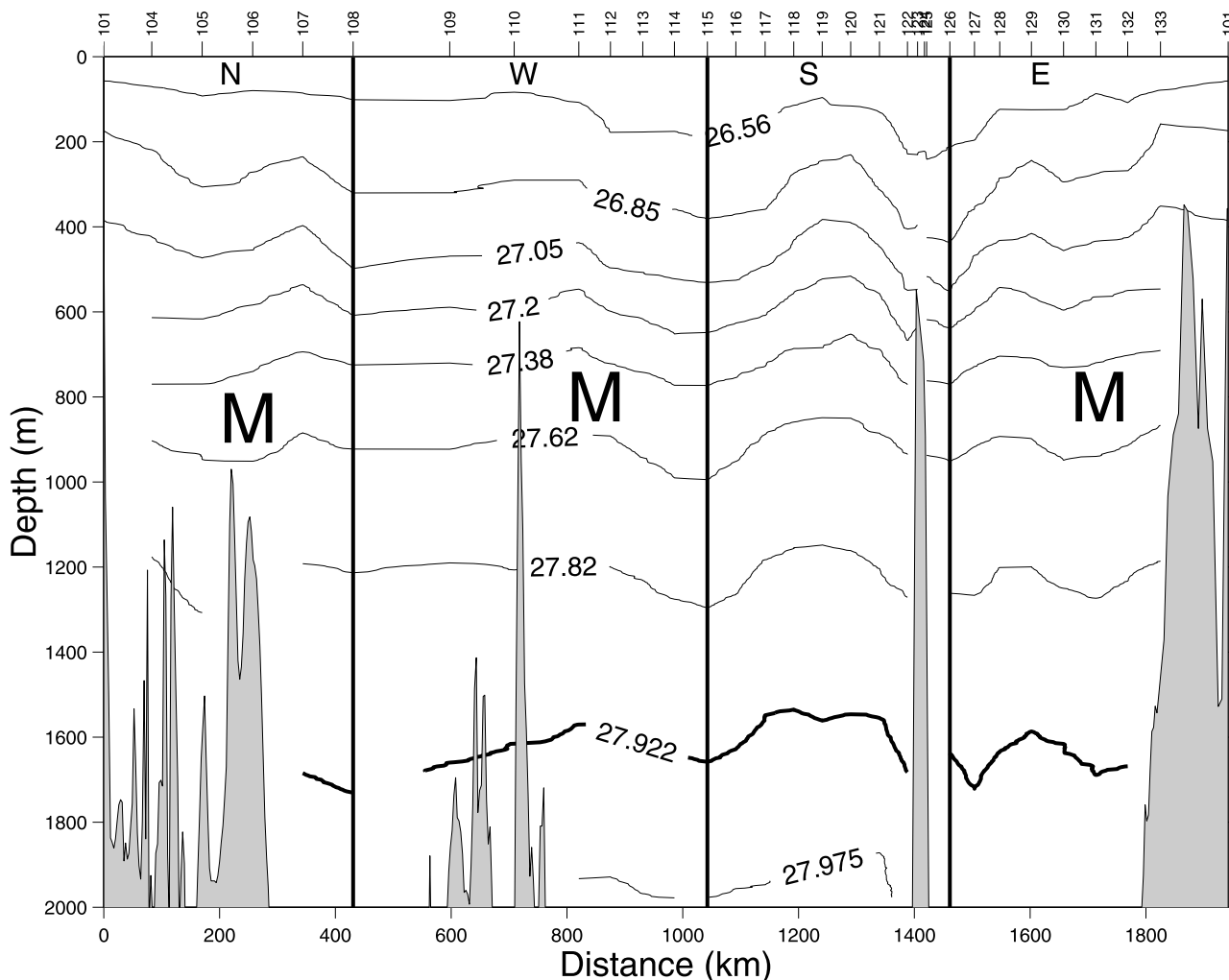


Figure 3. Isopycnals of neutral density (γ_n) along the cruise box. The 27.922 isopycnal is taken as the reference level for inverse model computation. Upper ticks indicate the stations numbering, while black vertical lines indicate the limits of CTD sections. N, northern; W, western; S, southern; E, eastern; M, meddies.

for example, seeded in between altimeter tracks. To avoid unwanted jumps to another closest minimum two precautions are undertaken. First, the SLH derivative field is composed from three corresponding consecutive fields, summed with decreasing weights as we step back in time. Second, a limitation is imposed on the signal propagation speed, e.g., the next tracking point cannot move more than one grid point away from the previous meddy position. This limitation serves to avoid sudden jumps to another anticyclonic structure when, at a particular moment, the surface signature of a meddy becomes hardly visible. With 7-day AVISO time step, this means that we consider meddies to have propagation velocities not exceeding 4 cm s^{-1} . Most frequently observed velocities of meddy propagation usually do not reach this value. Still, more exclusive cases of short-period fast translations may occur, when a meddy can move with the speed of up to 10 cm s^{-1} [Richardson and Tychemsky, 1998]. To catch up with the meddy in this situation, a possibility is foreseen for a track to jump over up to three grid points (to the closest vorticity minimum), when the SLH second derivative at the tentative newly

found tracking point abruptly falls to less than 50% of its previous value.

3. In Situ Signatures of the Observed Meddies

[10] The general water structure and its spatial variability at the time of OPALINA cruise are investigated. *TS* diagrams show that the CTD stations can be grouped into those with lower salinities below the main thermocline and those with higher ones (Figure 4, gray and black dots, respectively). The first region (stations 101–109) encompasses the southwestern part of the Azores plateau and the area to the west of MAR, and the second one (stations 110–133) covers the region south of the Azores and east of MAR (Figure 2). This reflects the known MW distribution pattern [Richardson *et al.*, 2000]. In the inverse model each of the subregions is treated as an “independent” basin with its own conservation balance. Vertically, the water column is separated in two layers with independent conservation balances: the main thermocline layer ($26.800 < \gamma_n < 27.200$) of the North Atlantic Central Water (NACW), and

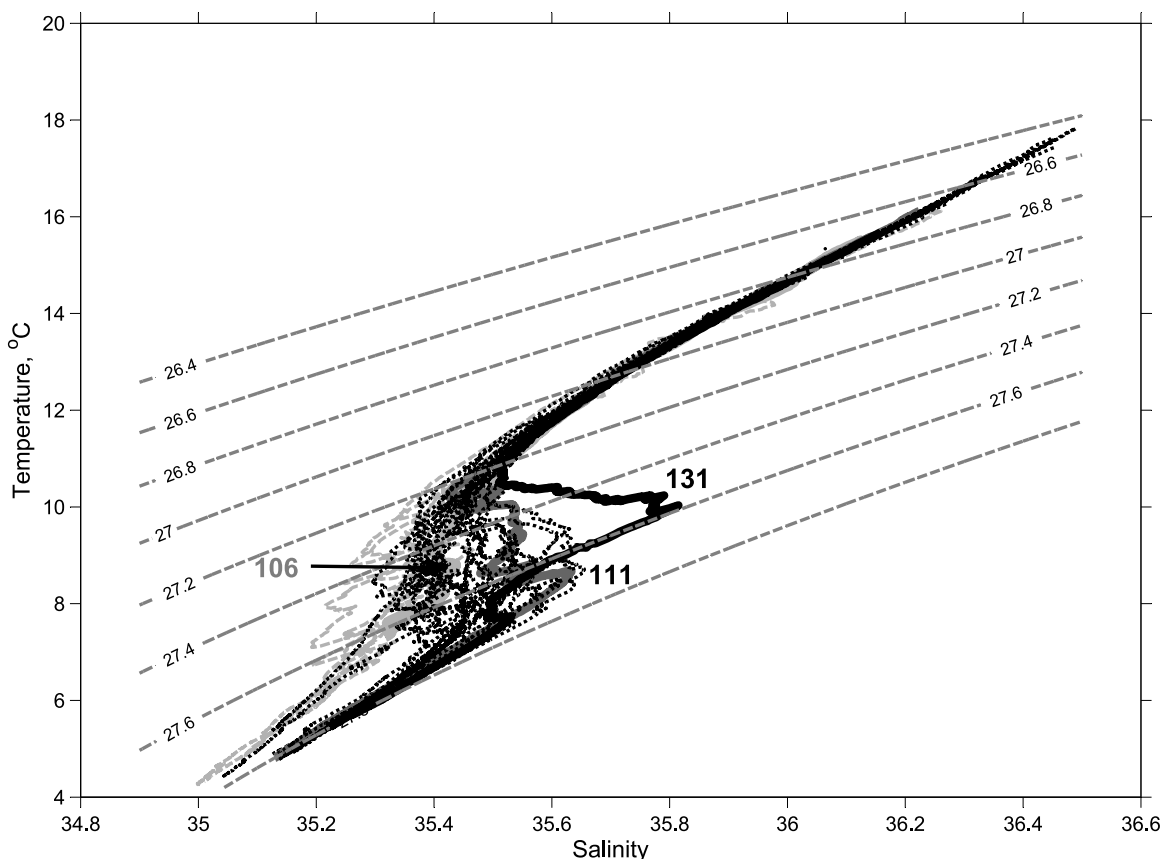


Figure 4. TS diagram for OPALINA cruise. The CTD stations from 101 to 108 are presented in gray, and the ones from 109 to 133 are presented in black. Thick lines are the casts inside the meddies M106 (light gray line), M111 (dark gray line), and M131 (black line). The σ_o density isolines are overlaid.

the intermediate level ($27.200 < \gamma_n < 27.922$) of the Subarctic Intermediate Water (SAIW), Mediterranean Water (MW) and Labrador Sea Water. As it is already discussed above, the base of the intermediate water level ($\gamma_n = 27.922$, at about 1600 m deep) is assumed to be the best choice for the reference level. At this level isopycnals have minimum tilt along the box boundaries (Figure 3), and computed v_o 's are small and stable along all the sections ($0.5 \pm 2 \text{ cm s}^{-1}$).

[11] The computed geostrophic currents are binned into five density layers (corresponding approximate depth layers are given in brackets): surface–26.85 (0–300 m), 26.85–27.20 (300–600 m), 27.20–27.62 (600–900 m), 27.62–27.82 (900–1200 m), 27.820–27.922 (1200–1600 m). The results showed that mass conservation is achieved in all the layers. The computed box-mean transport suggested a net eastward mass flux through the area at all the water levels, which primarily is a result of the eastward water transport by the AzC in the southern part of the region (Figure 5). Salt anomaly is not fully conserved in the surface layer (<300 m) and the upper MW layer (600–900 m). Aside of high possible error associated with salt flux computations; this may equally be a sign of unbalanced salt fluxes in and out of the region. Particularly, the inward salt flux across the eastern CTD section may be associated with the meddy entering the “box,” as discussed below. Water transport for the two meridional sections, obtained using the inverse model technique, is presented at Figure 6. In the southern

parts of the western and eastern sections an intensive eastward transport in the upper layer is associated with the AzC.

[12] The anticyclonic vortex, well pronounced in altimetry, has been crossed by the cruise track only in its eastern part. Even so, the CTD cast inside the vortex (station 131) demonstrates a pronounced positive salinity and temperature anomaly (0.4 psu and $2.0\text{--}2.5^\circ\text{C}$, respectively). The anomaly occupies the layer from 700 to 1000 m, with the maximum values at 900 m (Figures 4, 7a, 7b, and 7c). The salinity-temperature anomalies are coupled with low PV , and indicates that a meddy was crossed (M131). Figures 7a, 7b, and 7c also show, just below the meddy core, two high-salinity side-blobs. Those maxima stretch away from the core, perpendicular to the bottom slope (north of the meddy) and may be a result of meddy interaction with bottom topography. The anticyclonic rotation of the current vectors is centered at station 131, and extends up to the surface and down to the bottommost level (Figure 6).

[13] Besides M131, two other meddy-like structures have been observed. The one, centered at station 111 (M111), is characterized by moderate positive salinity and temperature anomalies (0.2 psu and $1.5\text{--}2.0^\circ\text{C}$, respectively), and a two-core structure (Figures 7d, 7e, and 7f). The main core, centered at 1000 m, corresponds to the region of comparatively low PV , though its minimum is shifted to the north. CTD-based geostrophic flows show the dynamic signature

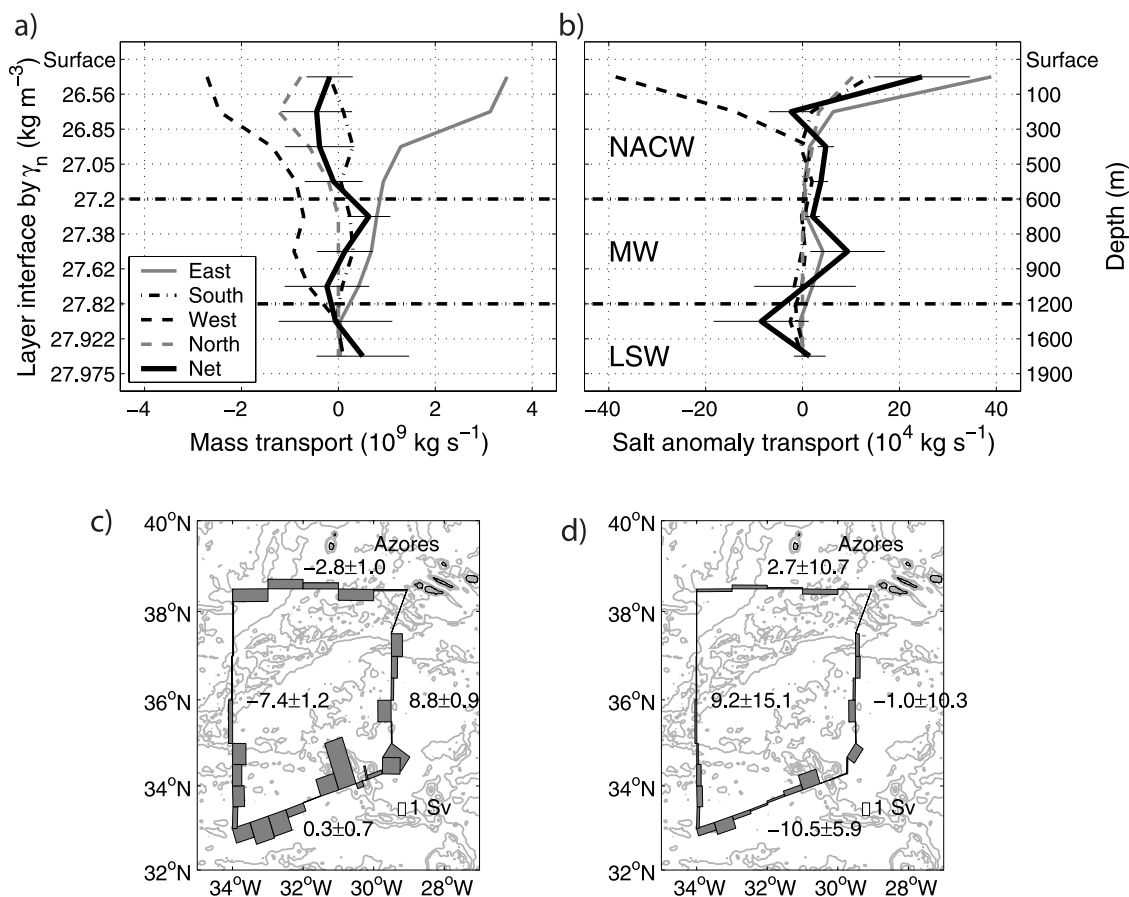


Figure 5. (a) Mass fluxes and (b) salt anomaly fluxes obtained with the inverse model for each of the CTD sections. The horizontal lines mark approximate borders of North Atlantic Central Water (NACW), Mediterranean Water (MW), and Labrador Sea Water (LSW), as used for computations. Mass fluxes obtained with the inverse model for (c) NACW ($\gamma_n < 27.200$) and (d) MW level ($\gamma_n < 27.820$). The computations are done for the reference level $\gamma_n = 27.922$. Numbers indicate mass transports in Sv through each of the section; for positive values the fluxes are outward from the box.

of the meddy to be disguised by the Azores front–current system (stations 111–115) and a southwestward mean flow between stations 110–111 (Figures 2 and 7). At the same time, in the segments of typical AzC influence (stations 112–114, as well as, 116–117 and 120–121 (not shown)), the ratios of the mean current speed in second to fourth vertical layers (300–600 m, 600–900 m and 900–1200 m) to the one in the upper layer (0–300 m) are about 60%, 45% and 20%, correspondingly. Between stations 111–112 the referred ratios are only 35%, 13% and 3%, respectively. This difference, most pronounced in the MW layer, we link to interaction with deep anticyclonic rotation around station 111, provoked by M111.

[14] Another meddy-resembling structure is associated with station 106 (M106). It has rather small positive salinity and temperature anomalies (0.10–0.15 psu and 1.0°C , respectively), and a pronounced negative *PV* anomaly (Figures 7g, 7h, and 7i). The core is situated between 700 and 1000 m depth, but the salinity anomaly extends throughout the water column (from the surface down to 1200–1400 m). Contrary to stations 105 and 107, where relative vorticity smoothly decreases away from the surface, at station 106 the temperature–salinity anomalies are associated with negative relative vorticity maximum in 300–900 m layer,

decreasing in absolute measure toward the surface and toward the bottom. Thus, both thermohaline and current patterns support the suggestion of meddy origin of the structure.

4. Remote Sensing Signatures of the Meddies

4.1. Altimetry Geostrophic Flows via in Situ

[15] Geostrophic currents derived from the altimetry observations (Figure 2) are compared with those obtained from the CTD sections. To be compatible, the altimetry currents were averaged and projected in the directions perpendicular to the CTD sections. Furthermore, we divided the eastern section into two segments (from stations 126 to 129 and from stations 129 to 133). The southern segment is the area of influence of the AzC and the northern one is that of the meddy M131. For both segments correlation between the altimetry and in situ currents is generally high throughout the water column. At the same time, for the southern segment the correlations are significant (at 5% significance level) only for the upper 600 m layer and decrease with depth, whereas for the northern segment the correlations increase with depth until reaching the significant maximum in the 600–1200 m layer. Similarly, for the depth-cumulative transports (e.g., the total transport from the sea surface to a

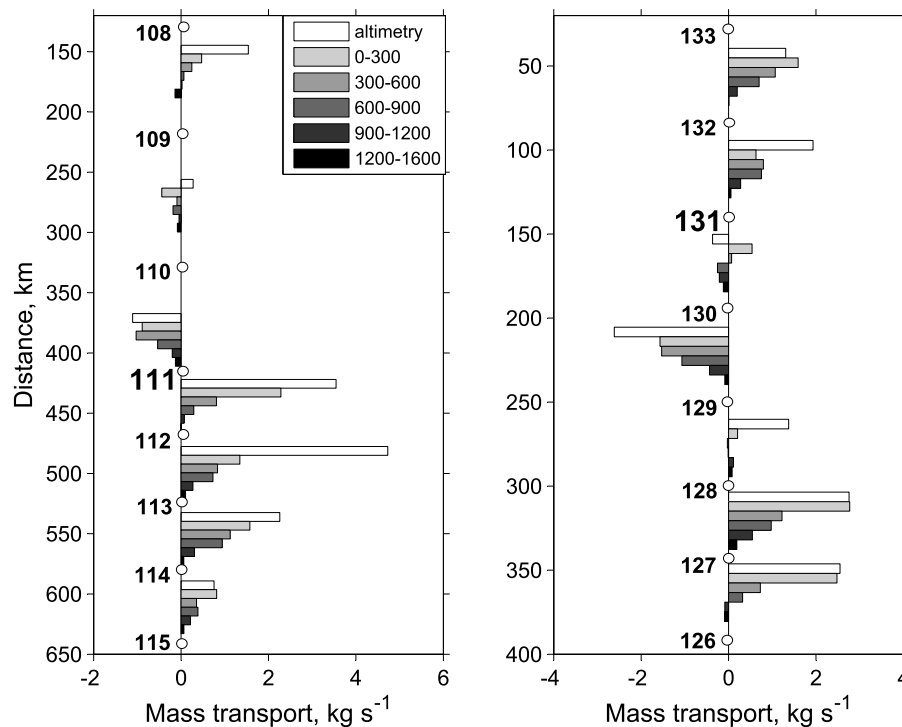


Figure 6. Geostrophic water transport (kg s^{-1}) across the cruise sections for different depth layers obtained from inverse modeling and altimetry data. (left) Western section, and (right) eastern section. Circles are the CTD the stations. Stations 111 and 131 are the closest to the centers of the corresponding meddies.

certain depth), the southern segment correlations reach maximum (100%) in the upper 600-m layer and gradually decrease with increasing layer thickness, while the northern segment correlations monotonically increase with increasing layer thickness. Though these correlations are derived from a small number of data-points, they are significant, stable and consistently changing, proving their validity.

[16] The results above suggest that the general current structure is similar throughout the whole 1600-m water column. However, over the meddy, the sea level variability reflects better the baroclinic flow structure at the intermediate water levels than those at the upper ones. This may result from the sea level topography being considerably affected by the barotropic component of the flow, correlated with the deep meddy structure. Equally, as an integral measure of the density structure throughout the water column, the sea level spatial variability may reflect the density anomalies in the intermediate or deep water layers, if those are dominating throughout the water column.

4.2. Surface Signature of Meddy M131, Traced Over 2 Years

[17] Figure 2 shows a clear altimetry signal of M131. The data suggest that the meddy center was located 30 to 60 km west of station 131, and the radius of its dynamic influence was around 160–180 km. With the method referred in the previous section, the anticyclonic structure could be traced forward to December 2005, and backward to October–December 2003 (Figure 8). After four months of stagnation to the northeast of the Josephine seamount, during February 2004, the meddy broke down with steady westward propagation. At the stagnation stage the meddy was difficult to

detect with altimetry, and its signature became more pronounced as it started its progress to the west. In December 2004 the meddy reached the Azores plateau, east of Santa Maria island. During the period of active movement, the M131 average propagation speed was about 2 km d^{-1} , e.g., typical for a meddy [Richardson *et al.*, 2000]. In January 2005 the meddy squeezed itself turning around the southern tip of the plateau, and regained a circular form west of Santa Maria in February. Then it started moving southwest along the southern flank of the plateau, generally following the 1000–2000 m isobaths. During June 2005 it trapped a substantial part of the AzC meander which made it much more visible on the surface. This is confirmed by our observations in July 2005: the ship thermometer registered a considerable increase in sea surface temperature of about $0.3\text{--}0.6^\circ\text{C}$ at both sides of the surface manifestation of M131 (Figure 9). Since then, the meddy slowly propagated southwest. In October 2005, after merging with another AzC meander, it was quickly translated south, crossing the AzC. At this stage it is very difficult to distinguish the meddy from the meander structures, solely on the basis of altimetry observations. In December 2005 the meddy had already crossed the AzC and was moving westward/southwestward, leaving the Atlantis seamounts to the east. The M131 trajectory is coherent with one of the previously reported major meddy paths [Shapiro and Meschanov, 1996; Richardson *et al.*, 2000].

[18] The suggested M131 path was checked against CTD-XBT data obtained from the NODC database [Boyer *et al.*, 2006]. Most of these profiles contain only temperature data and do not reach 900 m depth, limiting our analysis to temperature anomalies in the 600–800 m layer, where the

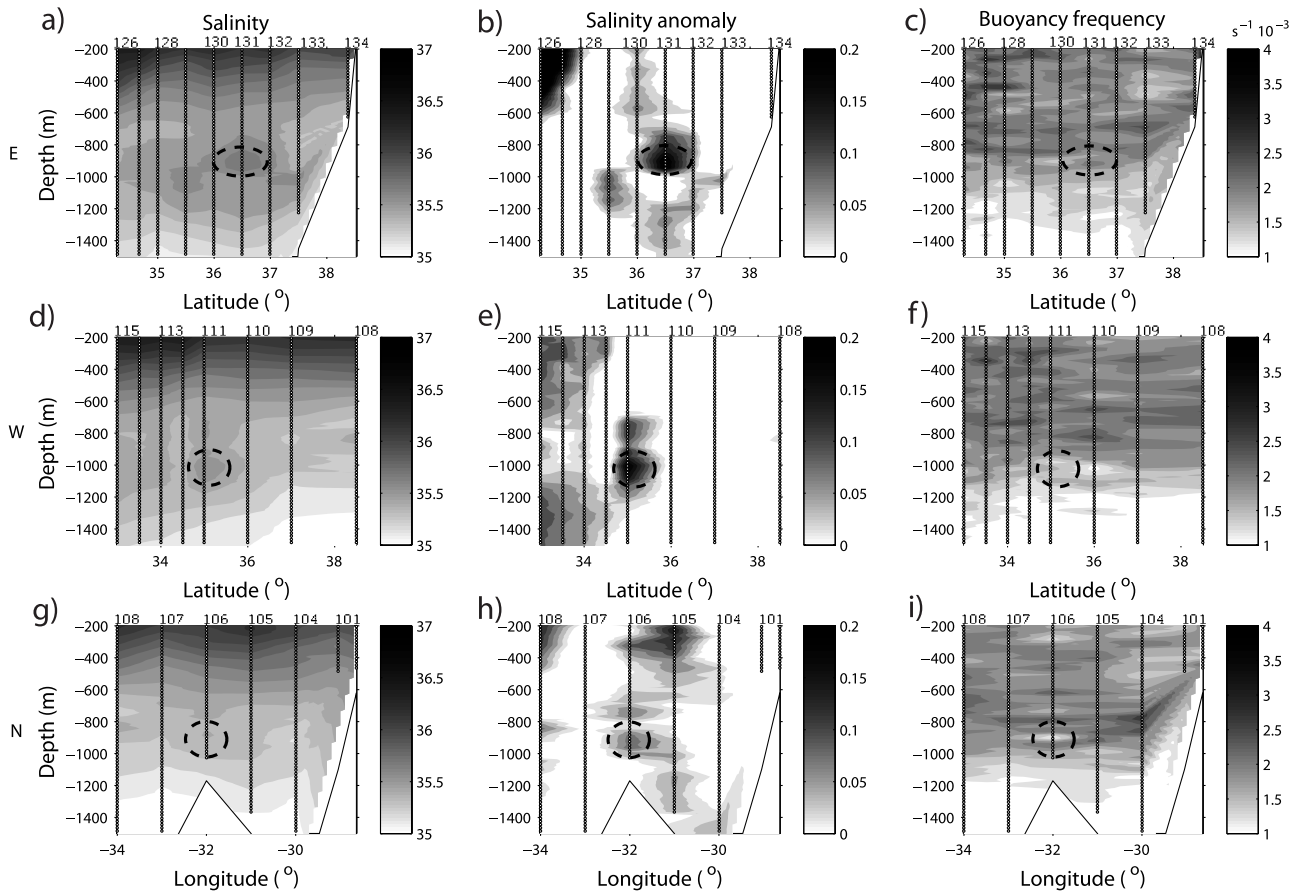


Figure 7. (a, d, g) Vertical cross section of salinity, (b, e, h) respective salinity anomalies, and (c, f, i) buoyancy frequency ($s^{-1} 10^{-3}$). The CTD sections (eastern (Figures 7a, 7b, and 7c), western (Figures 7d, 7e, and 7f), and northern (Figures 7g, 7h, and 7i)) are presented. Vertical lines and numbers above mark the CTD stations. The cores of meddies M131, M111, and M106, as crossed by the cruise, are marked with dashed ellipses. Lines below schematically represent the bottom topography.

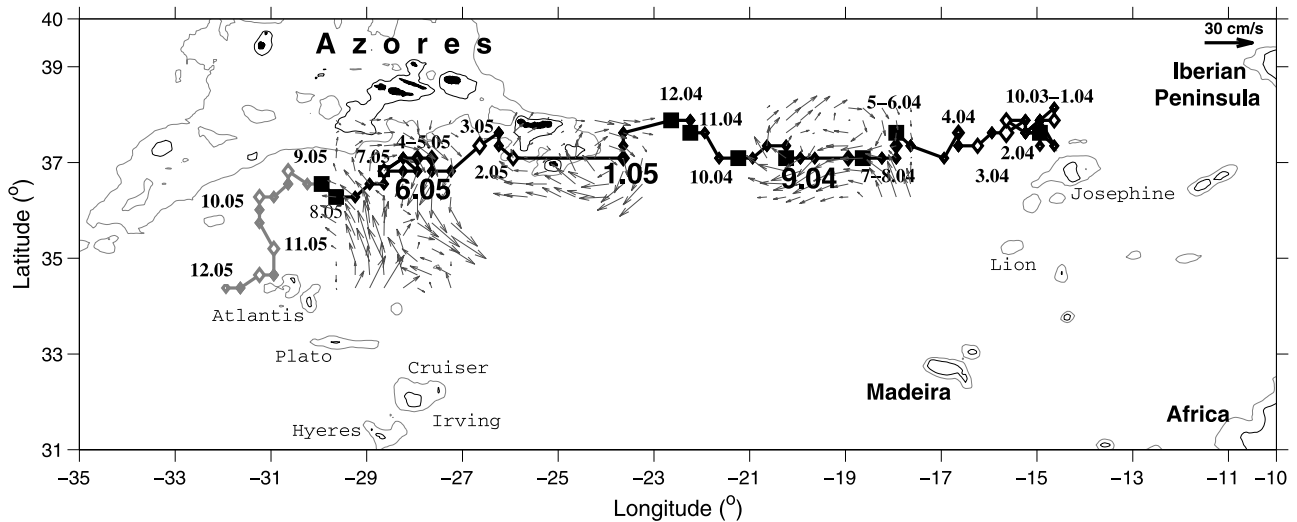


Figure 8. Tentative backward (black) and forward (gray) tracing of the M131 center estimated from altimetry data. Diamonds mark the beginning of a month and are labeled with corresponding month and year. Large squares represent the monthly mean positions where significant negative correlation between the in situ water temperature and the distance from the tentative meddy position is obtained. Altimetry currents over the meddy are plotted for the months marked in bold. Reference vector is also shown.

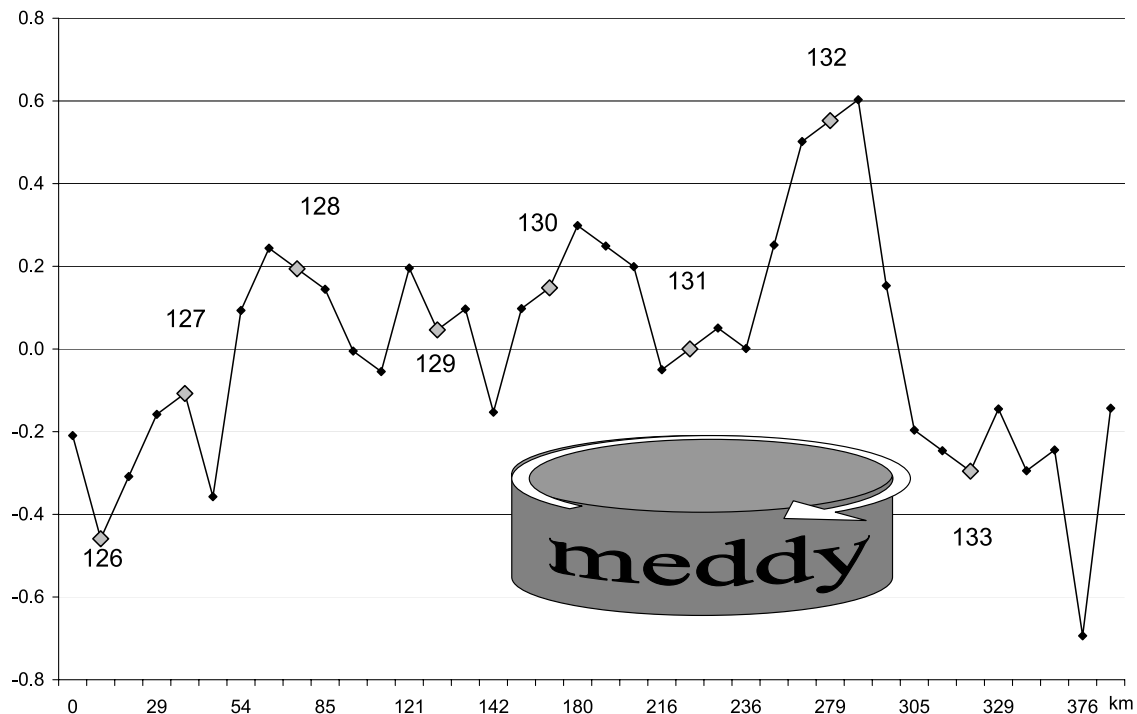


Figure 9. Ship-based sea surface temperature (3 m depth) along the eastern section, with the linear meridional trend excluded. Larger diamonds represent the measurements taken at CTD stations (see station names below). The upper scale is the distance from the beginning of the section (km).

meddy signal is quite weak. The anomalies are computed by subtraction from the individual casts the corresponding yearly climatic means, available from *Locarnini et al.* [2006]. The resulting temperature anomalies are concatenated into two parameters: the difference between temperature anomalies at 600 m and 800 m ($\Delta T = T_{800m} - T_{600m}$), and the integral of the temperature anomaly values between those two levels (T_{1int}). The later parameter is similar to the criteria “salinity anomaly of more than 0.4 psu over more than 200 m” used by *Richardson et al.* [1991] for in situ meddy detection. To prove their validity for meddy detection, the two parameters were tested against the data from OPALINA cruise (Figure 10a). Both ΔT and T_{1int} monotonically decrease with the distance from the meddy center and can be well approximated with logarithmic curves. The correlation between the logarithm of the distance from the meddy center (LDMC) and the parameters ΔT and T_{1int} are -66% and -92% , respectively, stable and significant. Similar parameters computed in the lower layers (T_{2int} in 800–1000 m and T_{3int} in 1000–1400 m), as well as, for salinity, gave correlations with LDMC between -85 and -95% . This proves that temperature data in the 600–800 m layer can be used to detect meddies.

[19] The method was applied for the temperature anomalies derived from the NODC data, on a monthly base and with several restrictions. First, we used only those temperature profiles for a corresponding month, which were in the radius of 350 km from the predicted monthly mean position of the meddy center. Second, we used only the profiles which passed or closely approached 800 m depth, integrated to 800 m or the deepest possible level. Third, to avoid confusion of meddy related anomalies with those of the upper ocean layer, T_{1int} was considered only if temperature

in the 600–800 m layer increased with depth ($\Delta T > 0$). With those limitations in mind, we analyzed 75 and 33 temperature profiles for 2004 and 2005, correspondingly. During 2005 the in situ casts were generally far from the meddy center and the correlations of T_{1int} with LDMC were low, reaching significant values only in January and June (-30 and -84% , respectively). The yearly mean correlation coefficient for 2004 was significant (-59% against 32%), and the parameters changed with the distance to the meddy center obeying the logarithmic law (Figure 10b). For monthly means, the significant values were reached in January, May, July, September, October, November and December 2004, with average correlations during those months of -70% . Especially strong correlation (-90%) was obtained for November 2004, when an XBT transect crossed the predicted meddy position. Thus, analysis of in situ data generally confirms that the predicted path corresponds to the M131 one.

4.3. Altimetry Signatures of Meddies M111 and M106

[20] Contrary to M131, clearly manifesting itself in altimetry, the M111 and M106 surface signals are difficult to identify (Figure 2). The difficulty partly arises from insufficiency of background in situ observations: the cruise track seems to just have touched a side of each of the vortices. We suppose that M111 is centered to the west of station 111 (around $34.8^\circ N$ and $34.5^\circ W$) and is responsible for the observed widening and bifurcation of the AzC meander, separated into two jets with noticeably different vertical structure (Figure 6). The correlation between altimetry and CTD derived geostrophic flows in the segment 110–113 is high throughout the water column, but reaches its maximum (98%) in the 600–1200 m layer. This contrasts with the

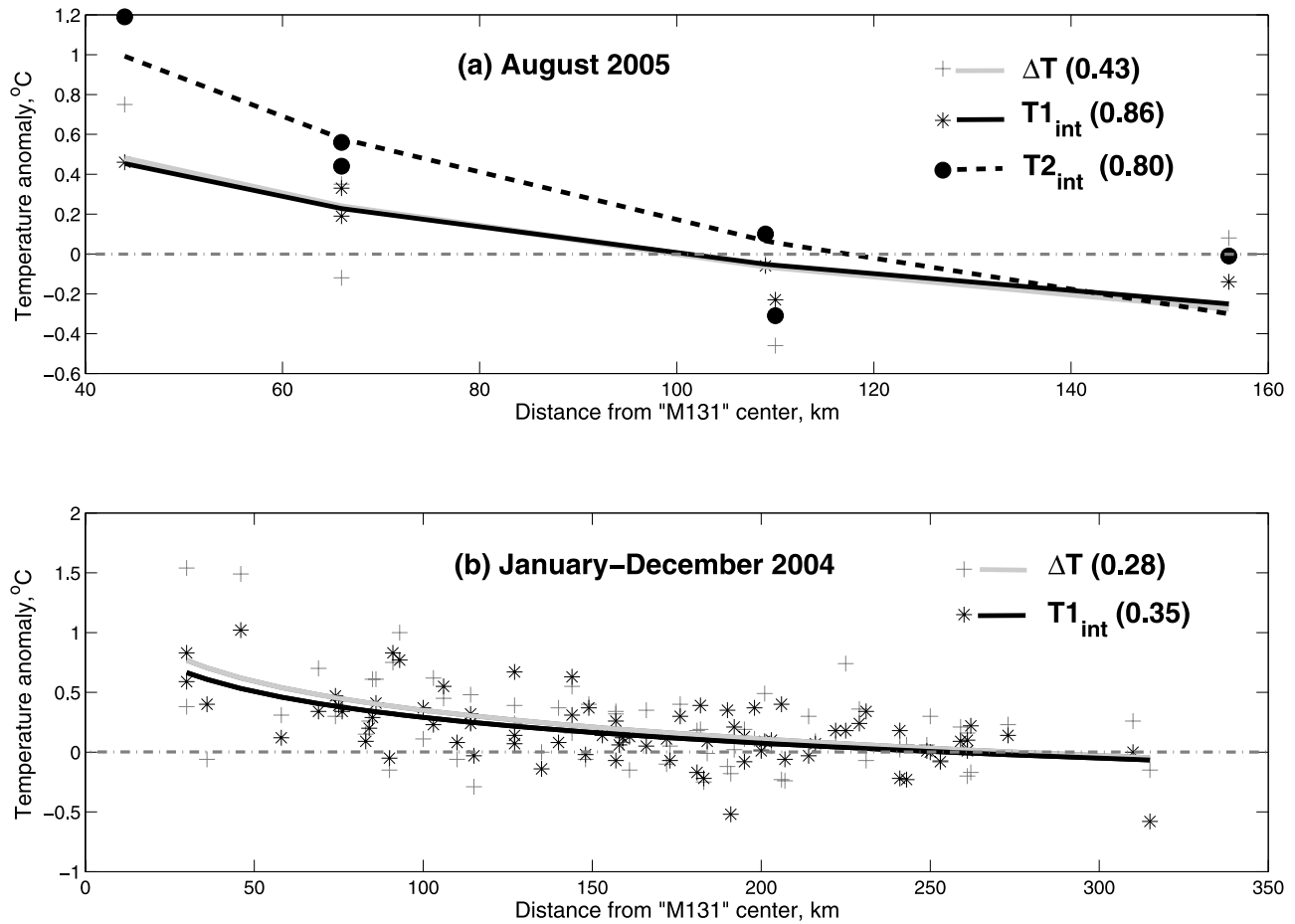


Figure 10. Dependence of ΔT (gray crosses) and $T_{1\text{int}}$ (black stars) with distance from the tentative/observed M131 center for (a) August 2005 (stations 128–133) and (b) January–December 2004. $T_{2\text{int}}$ (black dots) is the same as $T_{1\text{int}}$, but derived from temperature anomalies in 800–1000 m layer. The quality of the logarithmic fit (R^2) is given in brackets. Gray horizontal line marks zero temperature anomaly level.

vertical distribution of the correlations for the entire western and southern sections, decreasing with depth from 80–90% near the surface up to 70–80% at the MW level. Thus, M111 seems to affect the altimetry fields. The attempt to trace the meddy backward gave dubious results, since the signal is often interrupted by multiple interactions with AzC meanders.

4.4. Tracking Historic Meddies

[21] To test the consistency of the meddy-tracking methodology and its possible limitations, historical meddies,

tracked in situ with RAFOS floats, were followed with altimetry. The AVISO gridded data can be obtained since October 1992, when both, T/P and ERS-1 data became available. Therefore, we will mostly confine our study to the experiments of 1993–1997, when several meddies were followed with RAFOS floats for long periods of time [Richardson and Tychensky, 1998; Richardson *et al.*, 2000]. Characteristics of these meddies are summarized in Table 2.

[22] Hyperion, an intensive meddy, was discovered south of the Azores in July 1993 (Figure 1). It was traced forward

Table 2. Characteristics of Meddies Observed With RAFOS Floats^a

Reference	Meddy Name	Period of in Situ Observations	Core Depth (m)	dT ($^{\circ}\text{C}$)	dS (psu)	Rr (km)
Richardson and Tychensky [1998]	Hyperion	24 Jul 1993 to 15 Jan 1995	850	3.0	0.8	60–120
	Zoe (M4)	9 Sep 1994 to 23 Feb 1995	950	2.4	0.6	100
	Encelade	12 Nov 1993 to 15 Oct 1994	950	4.0	0.9	70–150
	Ceres	28 Jul 1993 to 13 Feb 1994	950	1.2	0.4	50–100
Richardson <i>et al.</i> [2000] and Pingree [1995, 2002]	Pinball (Meddy 13)	4 Jan 1994 to 25 Dec 1994	950	1.0	0.3	80–120
Paillet <i>et al.</i> [2002]	Ulla	15 Apr 1997 to 18 Oct 1998	1000	2.5	0.5	5–65
This paper	M131	20 Aug 2005	900	>2.5	>0.4	-

^aHere dT is temperature anomaly, dS is salinity anomaly of the core, and Rr is radius of RAFOS floats rotations.

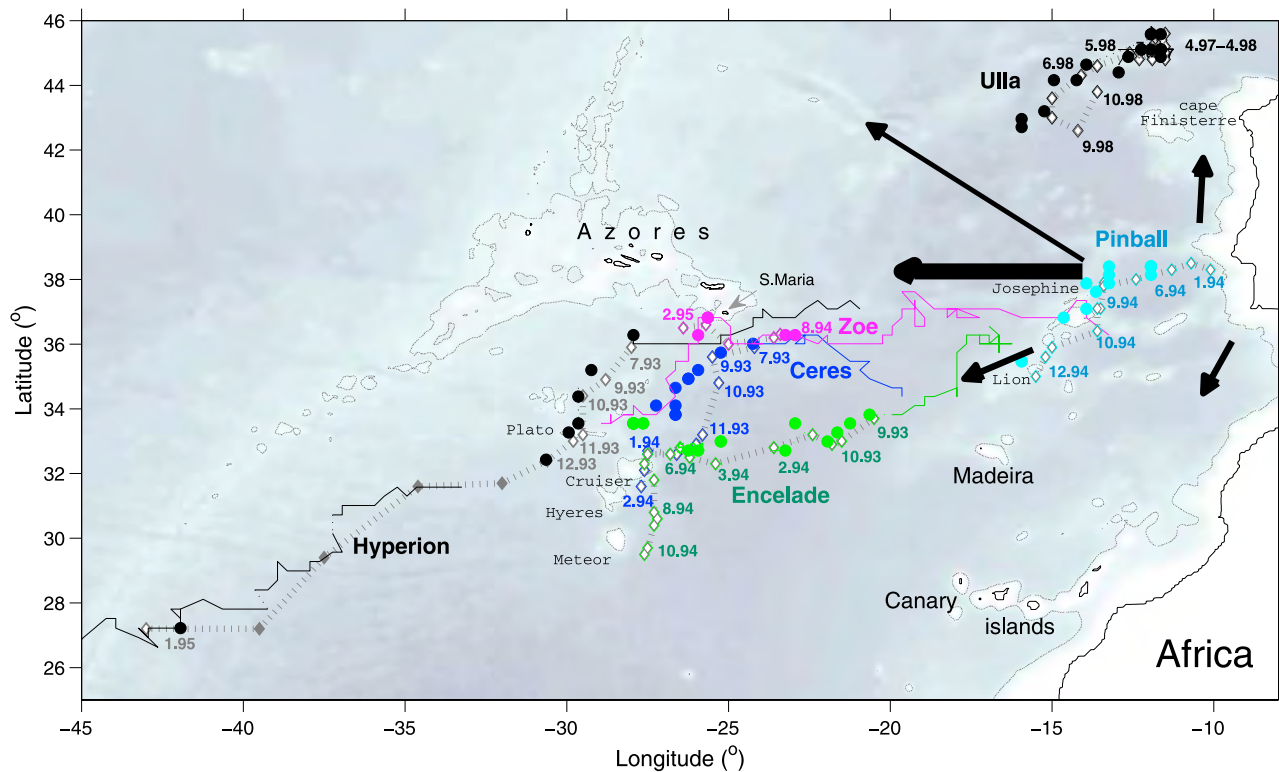


Figure 11. Remotely tracked meddies previously observed with RAFOS floats [Richardson *et al.*, 2000]. The empty diamonds, connected with gray dashed lines, represent in situ tracked meddies centers at a certain date (only month and year are specified). The closest dots of the same color are the respective positions of the tracked surface vortex centers. Black represents Hyperion, magenta represents Zoe, blue represents Ceres, green represents Encelade, cyan represents Pinball, and black also represents Ulla. When the two lines diverge, it means that the meddy signal is lost. Color lines represent forward/backward tracking of the corresponding meddies with altimetry, when no in situ observations are available. The meddies major pathways form [Shapiro and Meschanov, 1996] are represented with thick black arrows.

with RAFOS floats for 18 months, until it reached MAR around 27°N [Richardson and Tychensky, 1998; Richardson *et al.*, 2000]. We could safely track the meddy with its altimetry surface signal from July to September 1993, when finally it got aligned with the AzC anticyclonic meander (Figure 11, black track). In October 1993 the meddy became deeply embedded in the meander, and then made a sudden rapid translation to the south, having covered 120 km in 20 days (average speed of 5 cm s^{-1}). During this period it did not completely lose the surface signature, but it became difficult to follow it because of the AzC vorticity patterns. At the end of October the tracking could be continued from a new position south of the Azores front. During October–November the meddy passed over the Plato seamount. At this point the RAFOS float stopped rotating and showed a sudden drop of temperature, and after passing the seamount continued its rotation, but with bigger radius [Richardson *et al.*, 2000]. This suggested some disruption of the meddy core, which, although, was not accompanied by any substantial weakening of the surface signature. The surface signal passed west of the Plato peak, while RAFOS followed along its eastern flank, which may imply either some tilting due to interaction with the AzC, or the meddy splitting and further remerging (Figure 1). The

next interruption of the surface track occurred 3 months later when the meddy got coupled with a strong cyclonic eddy (probably a “Storm” type [Pingree, 2002]). The loss of the track corresponded to fast meddy translation around the cyclonic eddy in the counterclockwise direction. Then, the meddy signal, with three interruptions, was followed for 17 months, until RAFOS surfaced in January 1995. At this point the floats had been rotating for about 3 weeks at the surface [Richardson and Tychensky, 1998], accompanied by a very clear dynamic signature of the meddy. By the end of this period a branch of surface current protruded from the north, obscuring the altimetry signal and having washed the RAFOS away. Still we were able to follow the anticyclonic structure moving westward, for at least another 3 months. Hyperion was also safely tracked backward for about 10 months, to 20°W.

[23] Zoe (Meddy 4) was another intensive meddy (Figure 11, magenta track), followed with RAFOS floats for 5 months southeast of the Azores islands [Richardson and Tychensky, 1998]. Again its signature was very clear and the track could be very closely followed with altimetry up to the moment of RAFOS surfacing and further on for a total period of 9 months. In June–July 1995 its surface signal merged an anticyclonic meander of the AzC and got

obscured. Zoe could be very clearly backtracked until January 1994. During this period of time, it steadily moved westward along 36°N with a speed of 4 cm s⁻¹. This period was preceded by a period of “stagnation,” accompanied by chaotic movement around the same position, probably because of interaction with other eddy structures. Again, during the stagnation period the meddy signal was not clearly seen in altimetry. Still we believe that the surface signature was recovered in October 1993 and could be tracked backward up to Josephine seamount. During June 1993, the meddy skirted round the northern edge of the seamount on its way out of the Iberian basin. Earlier meddy surface manifestations were interruptible and difficult to follow.

[24] Ceres at the time of observations was a rather modest meddy (Table 2) still clearly seen in altimetry (Figure 1). From the moment of RAFOS deployment in the core in July 1993, Ceres could be followed with altimetry for 4 months moving west and then south (Figure 11, blue line). During mid-October 1993, the meddy interacted with the AzC meander, and the RAFOS track showed fast meddy translation, with maximum speeds reaching 10 cm s⁻¹ [Richardson and Tychemsky, 1998]. At this point, the surface signal became intermittent, and after mid-November, no stable anticyclonic vorticity pattern over the RAFOS track could be obtained (Figure 1). This may be related with a growing weakness of the meddy, which three months later dissipated at Cruiser and Irving seamounts [Richardson *et al.*, 2000]. A very interesting picture could be obtained by backtracking the meddy, which was followed back for about two months. During May 1993 the stagnation period was accompanied with a weakening of the surface signal. This, in turn, was preceded by quick northward translation of the signal by an AzC cyclone in March 1993. This strong cyclone, itself, represents an AzC recirculation generated by Ceres, while (during November 1993) the meddy entered AzC meander, and for about one month partly blocked the AzC progress east at 20°W (Figure 1).

[25] Encelade represented an intensive meddy with strong temperature-salinity anomalies (Table 2), with, at times, quite clear surface signal (Figure 1). It was most difficult to follow with altimetry (Figure 11, green line), since during most of the period of the RAFOS tracking it progressed along the southern edge of the AzC, often masked by the dominating background negative vorticity. In May–June 1994 it finally bifurcated at Cruiser seamount into two equal-sized meddies [Richardson *et al.*, 2000]. Detailed study permitted to conclude, that the sporadic loss of the meddy track was due to insufficient accuracy of the tracking methodology and not the result of the complete loss of the signal. After bifurcation the altimetry signal followed more easily the stronger secondary meddy, which moved to the north and stayed trapped between the Cruiser and Plato seamounts. The meddy was back-traced to the southern tip of the Josephine seamount (January–February 1993). One signal loss during the tracking (June 1993), happened because of ambiguity of the vorticity structure just before the meddy merged with the AzC meander, coming from the north.

[26] Two meddies were traced Near the Iberian Peninsula, not far from the place of origin. Meddy Pinball [Pingree, 1995, 2002] was generated as a rather weak meddy in

January 1994 (Table 2). At the initial period of stagnation (January–June 1994) no stable surface signal of the meddy could be observed. The signal became apparent in May 1994, after Pinball started its propagation to the southwest (Figure 11, cyan). Since then, the RAFOS track could be closely followed with altimetry until the end of 1994, when the float left the meddy. During the comparatively short track from Lisbon canyon to Lion seamount, Pinball collided and merged first with Meddy-18 (July–August 1994), and then with Meddy-R (November–December 1994). During the Pinball collision with Meddy-18, both meddies could be seen as separate signals, merging together. The loss of RAFOS in November 1994 might be not a result of total dissipation of Pinball, but of expelling a part of its core [Richardson *et al.*, 2000]. During that time, altimetry showed Pinball signal passing between the Josephine and Lion seamounts to merge Meddy-R [Pingree, 2002]. The resulting meddy presumably experienced some months of stagnation and started a westward propagation only after merging with another meddy in May 1995.

[27] Tracking a rather intense meddy Ulla [Paillet *et al.*, 2002] was complementary to the previous discussion for three reasons. First, it was the only meddy tracked so far north (around 45°N, northwest of Cape Finisterre). Second, the meddy was tracked with RAFOS during 1997–1998, when T/P data (used solely for tracking all the meddies above), were complemented with the ERS-1 ones. Finally, the near-surface floats released over the meddy proved that it had a clear surface signal. In spite of those encouraging premises Ulla was difficult to follow with altimetry (Figure 1). During the initial period of stagnation, when the meddy went through a series of chaotic rapid movements around its initial position, the related surface signal was periodically lost, and the meddy could be followed only for the periods of 3–4 months (Figure 11, black line at the northeastern part of the map). After Ulla began a rapid movement to the south, the signal first got lost and then reappeared quite clearly in May 1998. Since then it could be tracked until August 1998. The final part of the RAFOS trajectory, to the east and back to the north, was performed by nearly nonrotating RAFOS, and did not correspond to any stable surface signature. Instead, in August 1998, the Ulla surface signal merged with another anticyclonic signal coming from the west, which might be another meddy. Then, the merged vortex continued to the southwest.

5. Discussion

[28] In agreement with previous studies, we have shown that the observed meddies manifest themselves at the surface as negative relative vorticity signals, which can be detected and followed with satellite altimetry. The signals persist throughout the whole water column above the meddy, as it has been previously observed with surface and sub-merged floats, moored current meters and geostrophic computations from hydrographic sections [Tychemsky and Carton, 1998; Paillet *et al.*, 2002; Siedler *et al.*, 2005]. Still the reasons for a deep ocean vortex to manifest itself on the surface remain unclear.

[29] Tychemsky and Carton [1998] suggested that surface manifestation of meddies (Ceres and Encelade) was due to alignment with anticyclonic surface eddies, particularly with

AzC meanders. In our case, manifestation of M131 also became more pronounced after it had interacted with the AzC (Figure 8). The interaction resulted in more intensive currents mainly at the outer edges of the meddy surface signature (Figure 6, station pairs 129–130 and 132–133). Closer to the meddy center (station pairs 130–131 and 131–132) the surface flows were not significantly affected and the velocity profiles peaked in 300–900m layer. Complementary, the data from the ship thermometer registered 0.3–0.6°C increase in the sea surface temperature to be confined to the outer edge of M131 (Figure 9). The CTD casts confirmed the sensible temperature increase at stations 130 and 132 (but not at 131), and followed it down to at least 200 m, though its weaker counterpart was detectable down to 500 m. Thus, a uniform trapped body of warm water, aligned with the meddy, which can be expected in the case of an anticyclonic AzC meander detachment, has not been observed. The surface water structure rather resembles the upper part of the Azores front being entrained into the intrinsic upper layer circulation above the meddy. This entrainment process can be observed with altimetry a bit earlier, during June 2005 (Figure 8). While tracing the vortex back in time, several events of similar trapping of different impinging flows can be detected. Following those events, the meddy surface signal enhances, but does not merge with another anticyclonic surface signals, nor deviates far away from the deep meddy core. Vertical alignment with the AzC meander usually takes place when the meddy approaches the AzC too close (M111 (Figure 2) and Hyperion, Encelade, and Ceres (Figure 1)). Typically, this ends with expelling the meddy south from the AzC (Hyperion, Ceres), but some meddies may stay in the AzC for many months (Encelade). Thus, we can conclude that, in general, dynamic manifestation of a meddy at the sea surface is not a result of its alignment with an upper layer anticyclonic vortex.

[30] Tracking a meddy with altimetry is possible because of existence of the accompanying sea level rise. For example, in the center of M131 (about 40 km west of station 131) the sea level anomaly reaches 10 cm. This agrees with the observations by *Oliveira et al.* [2000] for the meddies in Iberian basin. *Käse et al.* [1989] model of meddy generation out of a deep quasi-geostrophic jet shows that, even when the jet itself has no surface signal, the generated instabilities gain small surface signature of the order of 2 cm s⁻¹ already within 3 months after their formation have started. In another 3 months time, while the initially large bodies are fragmenting into several meddy-sized anticyclonic vortexes, the surface signal reaches 7 cm s⁻¹, which is around 70% of that at the MW layer (Table 1). In absence of horizontal density gradients in the upper layer, associated with the meddy surface signature, the cyclo-geostrophic balance is reached for the positive sea level anomaly over the meddy of about 3 cm. This SLH elevation is just above the precision of the altimetry measurements, but gives an important indication of the intrinsic character of a surface signature of a meddy. The model results go well with our observations of the surface signature formation over the meddy Pinballs which could be identified and tracked in altimetry only 4–6 months after its detachment from the Mediterranean undercurrent.

[31] Potentially, the sea level rise may result from lower mean density of the water column due to meddy presence.

Thus, the sea level slope across the AzC (between stations 126 and 128) is the result of the density change over the upper 1000 m of water column. For M131, the steric effect on the SLH may be estimated through comparison of the dynamic depth of the uppermost level at station 131 (DD_{131} , over the meddy) and the mean one of the closest stations 130 and 132 (DD_{av}). The computations showed that $DD_{131} - DD_{av}$ is positive over most of the water column, reaching its maximum at about 740 m, and then decreasing to the surface. The estimated sea level elevation over the meddy is 1 cm, which is one order less than the observed one. Thus, the sea level rise over the meddy is not of steric origin.

[32] Analysis of in situ data for meddy Ulla [*Paillet et al.*, 2002] revealed vertical velocity structure over the meddy to be different from the columnwise rotation. When going up from the meddy core to the sea surface, the radius of azimuthal velocity maximum widens from 15–25 to 25–30 km, the rotational period increases from 5–10 to 15–25 days. The rotation parameters get stabilized in the upper 400–500 m, where they better keep with the solid body rotation, than around the meddy core. This vertical structure suggests existence of two coupled vortexes: the meddy core and the vortex above. *Paillet et al.* [2002] speculated that the observed near-surface anticyclone is a result of the upper layer vortex tubes compression, generated by the meddy squeezing its way through the water column. If the generated upper layer vorticity is not compensated with a baroclinic adjustment, the unbalanced Coriolis force acts to horizontally converge the upper part of the water column, creating the associated surface rise, which can be observed in altimetry.

[33] On the basis of our in situ observations, we can estimate the components of the cyclogeostrophic balance equation [*Carton*, 2001] governing the rotation of the water layer above the M131 core. The approximation implies that the Coriolis force (F_c) directed to the vortex center is balanced with the outward directed pressure gradient (F_p) and centrifugal (F_{cf}) forces. Using the observed values of the upper layer thickness $h = 600$ m, the eddy radius $r = 50$ km, horizontal density change over and away from the meddy $\delta\rho = 0.04$ kg m⁻³, and normalizing all the forces by the mean water density, we obtain: $F_p = g h \delta\rho/r = 0.46 \cdot 10^{-5}$ m s⁻². The centrifugal force ($F_{cf} = v_\theta^2/r$) for the velocities of order of 0.10 m s⁻¹ does not reach 0.02 $\cdot 10^{-5}$ m s⁻² and is negligible. So we end with geostrophic approximation, where F_p is balanced with the Coriolis force: $F_p = F_c = f v_\theta$. From this equation we can obtain the baroclinic current velocity (v_θ) of order of 5 cm s⁻¹, which corresponds to the inverse model estimates. The change in the upper layer thickness due to meddy movement will also result in another type of circulation. The absolute vorticity conservation in the upper layer, $(\zeta + f)/h = \text{const}$, suggests that if the isopycnal at the top of the meddy core rises by $\delta h = 20$ m, the upper layer gains anticyclonic vorticity of $\delta\zeta = -0.03 f$, which generates azimuthal currents of about 15 cm s⁻¹. The associated circulation will be affected by the Coriolis force $F_c \sim 1.40 \cdot 10^{-5}$ m s⁻², which will act to converge the water above the meddy until it is balanced with the sea level pressure gradient force ($F_{ssh} = g \delta\eta/r$). The balance is reached when the sea level rise over the meddy ($\delta\eta$) attains 7 cm. This value is close to the one observed over the meddy in altimetry.

[34] If the conclusions above are correct, a direct consequence of a meddy effect on the sea level, while pushing itself through the water column, should be negative correlation between the speed of the meddy propagation and the height of the associated sea level rise (or vorticity), e.g., the faster the meddy moves, the stronger vorticity it generates in the upper layer. This dependence was tested for M131. The velocity of the meddy movement relative to the Earth was computed by dividing the distance between two consecutive meddy center positions with the corresponding time lag. The background currents were obtained by averaging altimetry flows in 1×1 to 4×4 degree squares, surrounding the meddy surface signal. Finally, the module of the meddy speed relative to the water was obtained as a result of corresponding vector subtracting. All the variables discussed were smoothed with 8-week median filter. The results show high and significant negative correlation between the relative speed of the meddy propagation and the associated surface vorticity signal. Depending on the square size the correlation coefficients vary between -50 and -60% .

[35] Comparison of several backtracks of the meddies monitored in this paper (Figures 8 and 11) show close agreement with the meddies pathways suggested by *Shapiro and Meschanov* [1996]. Namely, meddies Hyperion, Zoe and M131 took the major vein, skirting the Josephine seamount from the north and then propagating between 36 and 38°N toward the Azores archipelago. Encelade, Pinball and, probably, Ceres took the middle branch, skirting the Josephine seamount from the south and propagating between 34 and 36°N multiply interacting with the AzC.

6. Conclusions

[36] From the discussion above we can conclude that the SLH manifestation of a meddy at the sea surface is an intrinsic propriety of meddy dynamics. A moving meddy, while raising isopycnals, also compresses the vorticity tubes above. Both processes act to generate anticyclonic vorticity in the upper layer. Baroclinic adjustment is responsible for about a half of the resulting vorticity, while another half is due to barotropic adjustment.

[37] Our observations suggest that, away from the formation region, the surface dynamic signature of a meddy is sufficiently stable even for rather modest features (Pinball, Ceres, Ulla). It was possible to track several meddies with the related altimetry signals for several months, and, in favorable conditions, for more than 1 year. Our results from 1993–1994 (T/P satellite only), 1997 (T/P and ERS-1) and 2003–2005 (T/P, Jason-1, Envisat and GFO) do not show any major improvement in the length of uninterrupted meddy tracks for multisatellite missions as compared to a single satellite (T/P) mission. The earlier Geosat data permitted *Stammer et al.* [1991] to track meddy D for about 1 year. This suggests that one satellite on T/P orbit may be sufficient for the tracking.

[38] The major failures in meddy tracking may be separated into the “methodological” and “natural” ones. The methodological drawbacks account for the situation when a meddy signal becomes weak and/or further tracking is dubious because of presence of other negative vorticity

structures. The limitation on meddy propagation velocity ($<4 \text{ cm s}^{-1}$) accounts for most of the track losses, typically bind to temporary dilution of the surface signal during fast meddy translations, while it interacts with a topographic rise, intensive surface current or another vortex. Thus, interaction of Hyperion with a strong cyclone resulted in the meddy surface signal dilution and splitting during the short period of its rapid translation along the cyclone edge. Alignment with the AzC anticyclonic meanders, thought initially enhancing a meddy surface signal, disguises the moment when the meddy (even a strong one) is expelled from the current. Similarly, the surface signature of a meddy traveling along AzC current (Encelade), is easily confused with the negative vorticity structures related to the flow, and is difficult to follow. The methods, better taking into account meddy dynamics, should improve the situation.

[39] The natural problems arise when, under certain dynamic conditions, the surface signal completely disappears or splits. Ambiguity in signal tracking may arise from two meddies merging together (Pinball), or when a meddy splits into two equal-sized vortexes (Ceres). Merging is more characteristic for the meddy formation sites, while splitting is quite typical when a meddy interacts with a topographic rise [*Cenedese*, 2002]. Relative movement appears to be an important condition for a meddy to have a clear surface signature. Observations suggest that during the periods of stagnation the associated surface signals become weak and intermittent (Ulla, etc.). Disappearing of the surface signal may also come up when a weak, ready to dissipate, meddy (like Ceres) interacts with another dynamic structure (AzC).

[40] Enhancement of meddy surface signal usually is observed during the periods of its steady propagation. It also results from trapping of a part of a foreign frontal interface (M131), or vertical alignment with another vortex (Ceres).

[41] Finally, we would like to point out that the surface signal may not immediately overlay the meddy, but the vorticity tubes may be tilted by the background circulation. Thus, simultaneous sequences of negative vorticity signals in the MW and the upper ocean layers (Encelade) were obtained with floats by *Tychensky and Carton* [1998]. The results showed that while the meddy was entering the AzC from the north, the upper anticyclonic eddy became tilted upstream, forcing a meander formation. During this period, the altimetry-derived “meddy center” was typically located in between the lower and the upper vorticity minima. One month later the two structures were already vertically aligned, and altimetry signature pointed at the meddy core.

[42] The results of this work are encouraging since they suggest a possibility for long-term routine meddy tracking, once an altimetry anomaly is linked to a meddy. Nevertheless, they again bring forward the difficulty in distinguishing between meddy related surface signals and those of the other anticyclonic vortexes.

[43] **Acknowledgments.** The work is accomplished under project OPALINA (PDCTE/CTA/49965/2003), sponsored by the European Space Agency (ESA) and the Foundation for Science and Technology of Portugal (FCT). We would like also to acknowledge the scientific projects DETRA (Regional Direction of Fisheries (DRP)) and LAMAR (Regional Foundation for Science and Technology (DRCT-M2.1.2/F/008/2007)). We also thank a postdoctoral fellowship sponsored by DRCT together with Institute

of Marine Research (IMAR/DRCT/REF. U&D/MED.M1.1.2/008/2005//BPD/002/007) and a doctoral fellowship sponsored by DRCT together with University of the Azores (UAz/DRCT/REF. U&D/MED.M3.1.1/003/2005/A) for support of this work. We are especially grateful to the scientific and technical staff of R/V *Arquipelago* and IMAR-DOP/UAz, for help in preparation and accomplishment of the scientific mission. Special thanks are also due to Ana Filipa (IMAR-DOP/UAz) for help in altimetry data preparation. F. Machín is supported by the Juan de la Cierva Programme and CANOA Project (CTM2005–00444/MAR), both funded by the Spanish Ministry of Education and Science. We are also grateful for the anonymous reviewers, whose comments significantly added to the quality of the paper.

References

- Antonov, J. I., R. A. Locarnini, T. P. Boyer, A. V. Mishonov, and H. E. Garcia (2006), *World Ocean Atlas 2005*, vol. 2, *Salinity*, NOAA Atlas NESDIS, vol. 62, edited by S. Levitus, 182 pp., NOAA, Silver Spring, Md.
- Arhan, M., A. C. de Verdière, and L. Memry (1994), The eastern boundary of the subtropical North Atlantic, *J. Phys. Oceanogr.*, *24*, 1295–1316, doi:10.1175/1520-0485(1994)024<1295:TEBOTS>2.0.CO;2.
- Bashmachnikov, I., C. Mohn, J. L. Pelegrí, A. Martins, F. Machín, F. Jose, and M. White (2009), Interaction of Mediterranean Water eddies with Sedlo and Seine seamounts, subtropical Northeast Atlantic, *Deep Sea Res., Part II*, doi:10.1016/j.dsr2.2008.12.036, in press.
- Bower, A. S., L. Armi, and I. Ambar (1997), Lagrangian observations of meddy formation during a Mediterranean Undercurrent Seeding Experiment, *J. Phys. Oceanogr.*, *27*, 2545–2575, doi:10.1175/1520-0485(1997)027<2545:LOOMFD>2.0.CO;2.
- Boyer, T. P., J. I. Antonov, H. E. Garcia, D. R. Johnson, R. A. Locarnini, A. V. Mishonov, M. T. Pitcher, O. K. Baranova, and I. V. Smolyar (2006), *World Ocean Database 2005*, NOAA Atlas NESDIS, vol. 60, edited by S. Levitus, 190 pp., NOAA, Silver Spring, Md.
- Carton, X. (2001), Hydrodynamical modelling of oceanic vortices, *Surv. Geophys.*, *22*, 179–263, doi:10.1023/A:1013779219578.
- Cenedese, C. (2002), Laboratory experiments on mesoscale vortices colliding with a seamount, *J. Geophys. Res.*, *107*(C6), 3053, doi:10.1029/2000JC000599.
- Ganachaud, A. (2003), Large-scale mass transports, water mass formation, and diffusivities estimated from World Ocean Circulation Experiment (WOCE) hydrographic data, *J. Geophys. Res.*, *108*(C7), 3213, doi:10.1029/2002JC001565.
- Iorga, M. C., and M. S. Lozier (1999), Signature of the Mediterranean outflow from a North Atlantic climatology: 2. Diagnostic velocity fields, *J. Geophys. Res.*, *104*, 26,011–26,029, doi:10.1029/1999JC900204.
- Jackett, D. R., and T. J. McDougall (1997), A neutral density variable for the world's oceans, *J. Phys. Oceanogr.*, *27*, 237–263, doi:10.1175/1520-0485(1997)027<0237:ANDVFT>2.0.CO;2.
- Käse, R. H., and W. Zenk (1987), Reconstructed Mediterranean salt lens trajectories, *J. Phys. Oceanogr.*, *17*, 158–163, doi:10.1175/1520-0485(1987)017<0158:RMSLT>2.0.CO;2.
- Käse, R. H., A. Beckmann, and H. H. Hinrichsen (1989), Observational evidence of salt lens formation in the Iberian basin, *J. Geophys. Res.*, *94*, 4905–4912, doi:10.1029/JC094iC04p04905.
- Le Cann, B., M. Assenbaum, J. C. Gascard, and G. Reverdin (2005), Observed mean and mesoscale upper ocean circulation in the midlatitude northeast Atlantic, *J. Geophys. Res.*, *110*, C07S05, doi:10.1029/2004JC002768.
- Locarnini, R. A., A. V. Mishonov, J. I. Antonov, T. P. Boyer, and H. E. Garcia (2006), *World Ocean Atlas 2005*, vol. 1, *Temperature*, NOAA Atlas NESDIS, vol. 61, edited by S. Levitus, 182 pp., NOAA, Silver Spring, Md.
- Machín, F., A. Hernández-Guerra, and J. L. Pelegrí (2006), Mass fluxes in the Canary Basin, *Prog. Oceanogr.*, *70*(2–4), 416–447, doi:10.1016/j.pocean.2006.03.019.
- Maze, J. P., M. Arhan, and H. Mercier (1997), Volume budget of the eastern boundary layer off the Iberian Peninsula, *Deep Sea Res., Part I*, *44*, 1543–1574, doi:10.1016/S0967-0637(97)00038-1.
- Müller, T., and G. Siedler (1992), Multi-year current time series in the eastern North Atlantic Ocean, *J. Mar. Res.*, *50*, 63–98.
- Oliveira, P. B., N. Serra, A. F. G. Fiúza, and I. Ambar (2000), A study of meddies using simultaneous in-situ and satellite observations, in *Satellites, Oceanography and Society*, Elsevier Oceanogr. Ser., vol. 63, pp. 125–148, Elsevier, Amsterdam.
- Paillet, J., B. Le Can, X. Carton, Y. Morel, and A. Serpette (2002), Dynamics and evolution of a northern meddy, *J. Phys. Oceanogr.*, *32*, 55–79, doi:10.1175/1520-0485(2002)032<0055:DAEOAN>2.0.CO;2.
- Pedlosky, J. (1987), *Geophysical Fluid Dynamics*, 2nd ed., 710 pp., Springer, New York.
- Pingree, R. D. (1995), The droguing of Meddy Pinball and seeding with ALACE floats, *J. Mar. Biol. Assoc. U. K.*, *75*, 235–252.
- Pingree, R. D. (2002), Ocean structure and climate (eastern North Atlantic): In situ measurement and remote sensing (altimeter), *J. Mar. Biol. Assoc. U. K.*, *82*, 681–707, doi:10.1017/S0025315402006082.
- Pingree, R. D., and B. Le Cann (1993), A shallow meddy (a smeddy) from the secondary Mediterranean salinity maximum, *J. Geophys. Res.*, *98*, 20,169–20,185, doi:10.1029/93JC02211.
- Richardson, P. L., and A. Tychensky (1998), Meddy trajectories in the Canary Basin measured during the Semaphore Experiment, 1993–1995, *J. Geophys. Res.*, *103*, 25,029–25,045, doi:10.1029/97JC02579.
- Richardson, P. L., D. Walsh, L. Armi, M. Schröder, and J. F. Price (1989), Tracking three meddies with SOFAR floats, *J. Phys. Oceanogr.*, *19*, 371–383, doi:10.1175/1520-0485(1989)019<0371:TTMWSF>2.0.CO;2.
- Richardson, P. L., M. S. McCartney, and C. Maillard (1991), A search for meddies in historical data, *Dyn. Atmos. Oceans*, *15*, 241–265, doi:10.1016/0377-0265(91)90022-8.
- Richardson, P. L., A. S. Bower, and W. Zenk (2000), A census of meddies tracked by floats, *Prog. Oceanogr.*, *45*(2), 209–250, doi:10.1016/S0079-6611(99)00053-1.
- Schultz Tokos, K., H. H. Hinrichsen, and W. Zenk (1994), Merging and migration of two meddies, *J. Phys. Oceanogr.*, *24*, 2129–2141, doi:10.1175/1520-0485(1994)024<2129:MAMOTM>2.0.CO;2.
- Serra, N., and I. Ambar (2002), Eddy generation in the Mediterranean undercurrent, *Deep Sea Res., Part I*, *49*, 4225–4243, doi:10.1016/S0967-0645(02)00152-2.
- Shapiro, G. I., and S. L. Meschanov (1996), Spreading pattern and mesoscale structure of Mediterranean outflow in the Iberian basin estimated from historical data, *J. Mar. Syst.*, *7*, 337–348, doi:10.1016/0924-7963(95)00011-9.
- Siedler, G., and R. Onken (1996), Eastern recirculation, in *The Warm Water Sphere of the North Atlantic Ocean*, edited by W. Krauss, pp. 339–364, Gebrüder Borntraeger, Berlin.
- Siedler, G., L. Armi, and T. J. Müller (2005), Meddies and decadal changes at the Azores front from 1980 to 2000, *Deep Sea Res., Part II*, *52*, 583–604, doi:10.1016/j.dsr2.2004.12.010.
- Stammer, D., H. H. Hinrichsen, and R. H. Käse (1991), Can meddies be detected by satellite altimetry?, *J. Geophys. Res.*, *96*, 7005–7014, doi:10.1029/90JC02740.
- Tournadre, J. (1990), Sampling oceanic rings by satellite radar altimeter, *J. Geophys. Res.*, *95*, 693–697, doi:10.1029/JC095iC01p00693.
- Tychensky, A., and X. Carton (1998), Hydrological and dynamical characteristics of Meddies in the Azores region: A paradigm for baroclinic vortex dynamics, *J. Geophys. Res.*, *103*, 25,061–25,079, doi:10.1029/97JC03418.
- Wunsch, C. (1996), *The Ocean Circulation Inverse Problem*, 442 pp., Cambridge Univ. Press, New York.

I. Bashmachnikov (corresponding author), A. Martins, and A. Mendonça, Institute of Marine Research, Department of Oceanography and Fisheries, University of the Azores, P-9901-862, Horta, Faial, Azores, Portugal. (igor@uac.pt)

F. Machín, Institut de Ciències del Mar, CSIC, Passeig Marítim de la Barceloneta 37-49, E-08003 Barcelona, Spain.